

**Spin fluctuations in  $\text{Sr}_{1.8}\text{La}_{0.2}\text{RuO}_4$** 

Zheng He,<sup>1</sup> Qisi Wang<sup>1,2,\*</sup>, Yu Feng,<sup>1,3,4</sup> Chul Kim,<sup>5</sup> Wonshik Kyung<sup>6,7</sup>, Changyoung Kim,<sup>6,7</sup> Hongliang Wo<sup>1,8</sup>, Gaofeng Ding,<sup>1,8</sup> Yiqing Hao,<sup>1</sup> Feiyang Liu,<sup>1</sup> Helen C. Walker<sup>9</sup>, Devashibhai T. Adroja<sup>9,10</sup>, Astrid Schneidewind<sup>11</sup>, Wenbin Wang,<sup>12</sup> and Jun Zhao<sup>1,12,8,13,†</sup>

<sup>1</sup>State Key Laboratory of Surface Physics and Department of Physics, Fudan University, Shanghai 200433, China

<sup>2</sup>Department of Physics, The Chinese University of Hong Kong, Shatin, Hong Kong, China

<sup>3</sup>Institute of High Energy Physics, Chinese Academy of Sciences (CAS), Beijing 100049, China

<sup>4</sup>Spallation Neutron Source Science Center (SNSC), Dongguan 523803, China

<sup>5</sup>Institute of Physics and Applied Physics, Yonsei University, Seoul 03722, Korea

<sup>6</sup>Center for Correlated Electron Systems, Institute for Basic Science, Seoul 08826, Korea

<sup>7</sup>Department of Physics and Astronomy, Seoul National University, Seoul 08826, Korea

<sup>8</sup>Shanghai Qi Zhi Institute, Shanghai 200232, China

<sup>9</sup>ISIS Facility, STFC Rutherford Appleton Laboratory, Chilton, Didcot, Oxfordshire OX11 0QX, United Kingdom

<sup>10</sup>Highly Correlated Matter Research Group, Physics Department, University of Johannesburg, P.O. Box 524, Auckland Park 2006, South Africa

<sup>11</sup>Jülich Centre for Neutron Science (JCNS) at Heinz Maier-Leibnitz Zentrum (MLZ), Forschungszentrum Jülich GmbH, Lichtenbergstr.1, 85748 Garching, Germany

<sup>12</sup>Institute for Nanoelectronic Devices and Quantum Computing, Fudan University, Shanghai 200433, China

<sup>13</sup>Shanghai Research Center for Quantum Sciences, Shanghai 201315, China



(Received 12 December 2021; revised 23 March 2023; accepted 5 April 2023; published 9 May 2023)

We use inelastic neutron scattering to study spin fluctuations in  $\text{Sr}_{1.8}\text{La}_{0.2}\text{RuO}_4$ , where Lanthanum doping triggers a Lifshitz transition by pushing the van Hove singularity in the  $\gamma$  band to the Fermi energy. Strong spin fluctuations emerge at an incommensurate wave vector  $\mathbf{Q}_{ic} = (0.3, 0.3)$ , corresponding to the nesting vector between  $\alpha$  and  $\beta$  Fermi sheets. The incommensurate antiferromagnetic fluctuations shift toward  $(0.25, 0.25)$  with increasing energy up to  $\sim 110$  meV. By contrast, scatterings near the ferromagnetic wave vectors  $\mathbf{Q} = (1, 0)$  and  $(1, 1)$  remain featureless at all energies. This contradicts the weak-coupling perspective that suggests a sharp enhancement of ferromagnetic susceptibility due to the divergence of density of states in the associated  $\gamma$  band. Our findings imply that ferromagnetic fluctuations in  $\text{Sr}_2\text{RuO}_4$  and related materials do not fit into the weak-coupling paradigm, but instead are quasilocal fluctuations induced by Hund's coupling. This imposes significant constraints for the pairing mechanism involving spin fluctuations.

DOI: [10.1103/PhysRevB.107.L201107](https://doi.org/10.1103/PhysRevB.107.L201107)

The pairing mechanism of the  $\text{Sr}_2\text{RuO}_4$  superconductor has been the focus of tremendous research activities [1–4], but as yet remains a mystery. For a long time,  $\text{Sr}_2\text{RuO}_4$  has stood as a promising candidate for a spin-triplet superconductor with a chiral  $p$ -wave order parameter [5–7]. A series of experiments supported this belief. Early on, nuclear magnetic resonance (NMR) [8] and polarized neutron diffraction [9] measurements show an unchanged magnetic susceptibility across the superconducting transition temperature ( $T_c$ ), suggesting an odd pairing state. In addition, a spontaneous time-reversal symmetry breaking at  $T_c$  has been observed by muon spin relaxation [10] and polar Kerr effect [11] studies, which reveals a chiral character of the superconducting state.

However, some experimental data such as the absence of edge currents [12,13], the Pauli-limited upper critical

field [14], and the lack of a linear strain dependency of  $T_c$  at zero strain limit [15] cannot be readily explained in this scenario. Furthermore, recent NMR [16,17] and polarized neutron diffraction [18] investigations revealed that the spin susceptibility in  $\text{Sr}_2\text{RuO}_4$  decreases significantly below  $T_c$ —contradicting a simple spin-triplet Cooper pairing. The discrepancies between these results have kicked off a flurry of studies to identify its pairing symmetry, and different composite order parameters have been put forward to reconcile the controversies [19–27]. Yet, the debate on this topic remains far from closed.

Superconductivity in  $\text{Sr}_2\text{RuO}_4$  arises near magnetic instabilities [28–30], as it does in cuprates and iron pnictides. As a result, spin fluctuations are believed to be critical for the Cooper pairing [31–35]. Theoretically, antiferromagnetic and ferromagnetic fluctuations could cause even and odd parity of superconducting order parameters, respectively [32,33]. Previous inelastic neutron scattering (INS) experiments on  $\text{Sr}_2\text{RuO}_4$  revealed strong two-dimensional incommensurate antiferromagnetic responses around wave

\*qwang@cuhk.edu.hk

†zhaoj@fudan.edu.cn

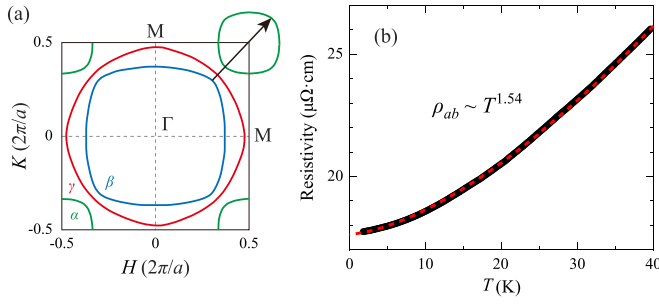


FIG. 1. (a) Schematic of the Fermi surfaces in the first Brillouin zone of  $\text{Sr}_{2-y}\text{La}_y\text{RuO}_4$  close to the Lifshitz transition, inferred from ARPES measurements [47]. Green, blue, and red solid curves represent  $\alpha$ ,  $\beta$ , and  $\gamma$  Fermi sheets, respectively. Black arrow indicates the nesting vector between  $\alpha$  and  $\beta$  bands. (b) In-plane resistivity  $\rho_{ab}$  versus temperature  $T$  in  $\text{Sr}_{1.8}\text{La}_{0.2}\text{RuO}_4$ . Red dashed curve is a powerlaw fitting  $AT^n + \rho_0$  with  $n = 1.54 \pm 0.04$ .

vector  $\mathbf{Q}_{ic} = (0.3, 0.3, L)$  and equivalent positions [36–43], which are attributed to the Fermi surface nesting between the quasi-one-dimensional  $\alpha$  and  $\beta$  sheets associated with the  $d_{xz}$  and  $d_{yz}$  orbitals, respectively [see Fig. 1(a)]. Meanwhile, weak magnetic fluctuations appear near the Brillouin zone center [38, 41, 43], manifesting a ferromagnetic character. The ferromagnetic fluctuations have been attributed to the nesting of  $\gamma$  bands [44, 45], but recent dynamical mean-field theory (DMFT) calculations instead suggested that the ferromagnetic fluctuations are quasilocal due to Hund’s coupling [46]. Yet, the origin of the ferromagnetic fluctuations is still under debate.

Band structure studies of  $\text{Sr}_2\text{RuO}_4$  reveal a van Hove singularity (vHS) in the  $\gamma$  band closely ( $\sim 49$  meV) above the Fermi level [44, 45, 47, 48]. Modest external perturbations can therefore significantly influence the Fermi surface topology and electronic properties [15, 45, 48–52]. For example, applying uniaxial strain on  $\text{Sr}_2\text{RuO}_4$  may induce a Lifshitz transition by pushing the vHS to the Fermi level and enhance  $T_c$  [50, 51]. Carrier doping by chemical substitution provides an alternative path to tune the electronic properties. For example,  $\text{La}^{3+}$  substitution for  $\text{Sr}^{2+}$  induces electron doping and generates a Lifshitz transition at the critical doping in  $\text{Sr}_{2-y}\text{La}_y\text{RuO}_4$  ( $y_c = 0.2$ ), where the vHS crosses the Fermi level [45, 47, 48]. A non-Fermi-liquid (NFL) behavior has been observed at the Lifshitz transition, manifesting the occurrence of a strong electronic renormalization and quasiparticle scatterings (see Fig. 1(b) and Ref. [45]). In the weak coupling scenario, the divergence of density of states near the vHS would greatly enhance the ferromagnetic spin fluctuations associated with the  $\gamma$  band [45], whereas quasilocal fluctuations are expected to be marginally affected and remain very weak [46]. The origin of ferromagnetic fluctuations in  $\text{Sr}_2\text{RuO}_4$  and related materials can thus be directly addressed by studying the  $\text{La}^{3+}$  doping effect.

In this paper, we report an INS study of spin fluctuations in  $\text{Sr}_{2-y}\text{La}_y\text{RuO}_4$  at the critical concentration  $y_c = 0.2$ , where the vHS in the  $\gamma$  band crosses the Fermi level. Strong incommensurate antiferromagnetic fluctuations are observed up to  $\sim 110$  meV and disperse from  $\mathbf{Q}_{ic} = (0.3, 0.3)$  to  $(0.25, 0.25)$ .

This differs from undoped  $\text{Sr}_2\text{RuO}_4$  where the antiferromagnetic fluctuations show little dispersion. On the other hand, no discernible ferromagnetic response has been detected with our experimental sensitivity. These results contradict the weak-coupling scenario that ferromagnetic fluctuations are induced by the nesting of the  $\gamma$  band; instead they support the proposal that magnetic responses near the ferromagnetic wave vectors have a quasilocal character.

High-quality  $\text{Sr}_{1.8}\text{La}_{0.2}\text{RuO}_4$  single crystals were synthesized using the floating zone method [53]. Electron probe micro analysis (EPMA) and x-ray diffraction (XRD) measurements are performed to confirm the chemical composition and characterize the quality of our sample. The XRD Rietveld refinement shows that  $\text{Sr}_{1.8}\text{La}_{0.2}\text{RuO}_4$  adopts the same space group ( $I4/mmm$ ) as  $\text{Sr}_2\text{RuO}_4$ . No impurity, disorder, or lattice distortion is detected (see the Supplemental Material [54]). Below 40 K, the in-plane resistivity follows a temperature dependence  $\rho_{ab} = AT^n + \rho_0$  with  $n = 1.54 \pm 0.04$  [Fig. 1(b)], deviating from the Fermi liquid behavior observed in undoped  $\text{Sr}_2\text{RuO}_4$ . This is consistent with previous reports [45]. Our INS experiments were carried out on the MERLIN time-of-flight spectrometer at the Rutherford Appleton Laboratory [56], and the cold triple-axis spectrometer PANDA at the Heinz Maier-Leibnitz Zentrum (FRMII) [57]. 21 pieces of single crystals with a total mass of  $\sim 12$  g were coaligned for the INS measurements. The time-of-flight experiment was performed with the incident neutron energies fixed at  $E_i = 18.8, 40.2$ , and  $135.8$  meV. Data were normalized to absolute units using the incoherent elastic scattering from a standard vanadium sample. Triple-axis experiments were performed with the final neutron energy fixed at  $E_f = 5.1$  meV. Pyrolytic graphite (002) [PG(002)] was used as a monochromator and analyzer. A Be filter was employed to reduce the contamination from higher-order neutrons. We define the wave vector  $\mathbf{Q}$  in the tetragonal unit cell at  $\mathbf{Q} = H\mathbf{a}^* + K\mathbf{b}^* + L\mathbf{c}^*$  as  $(H, K, L)$  in reciprocal lattice units (r.l.u.), where  $\mathbf{a}^* = 2\pi\hat{\mathbf{a}}/a$ ,  $\mathbf{b}^* = 2\pi\hat{\mathbf{b}}/b$ , and  $\mathbf{c}^* = 2\pi\hat{\mathbf{c}}/c$  with lattice parameters  $a = b = 3.86$  Å and  $c = 12.72$  Å.

Figure 2 displays constant-energy plots of the scattering intensity in the  $(H, K)$  plane at 5 K. At low energies [Figs. 2(a)–2(c)], clear scatterings are observed near the incommensurate wave vector  $\mathbf{Q}_{ic} = (0.3, 0.3)$  and equivalent positions. This is similar to the dominant antiferromagnetic spin fluctuations in  $\text{Sr}_2\text{RuO}_4$  [36, 37, 39]. It has been shown that La doping mostly influences the  $\gamma$  band, while the nesting condition between the  $\alpha$  and  $\beta$  Fermi sheets is weakly affected [47]. The scattering significantly weakens at the equivalent  $\mathbf{Q} = (0.7, 0.3)$  [Figs. 2 and 4(j)] due to the reduced  $\text{Ru}^{4+}$  magnetic form factor with increasing  $|\mathbf{Q}|$ , corroborating its magnetic origin. With increasing energy, the incommensurate peak positions move toward the lower  $\mathbf{Q}$  [Figs. 2(d)–2(i)], revealing a notable dispersion.

The dispersion of the incommensurate spin fluctuations can be better visualized in the contour plot of the  $E$ - $K$  plane. As illustrated in Fig. 3, strong spin fluctuations stem from  $\mathbf{Q}_{ic} = (0.3, 0.3)$  and disperse to  $(0.25, 0.25)$  around 110 meV. This behavior differs from  $\text{Sr}_2\text{RuO}_4$  where the peak position of spin fluctuations is essentially fixed at  $\mathbf{Q}_{ic}$  at all energies [39]. This difference indicates that La doping may induce a

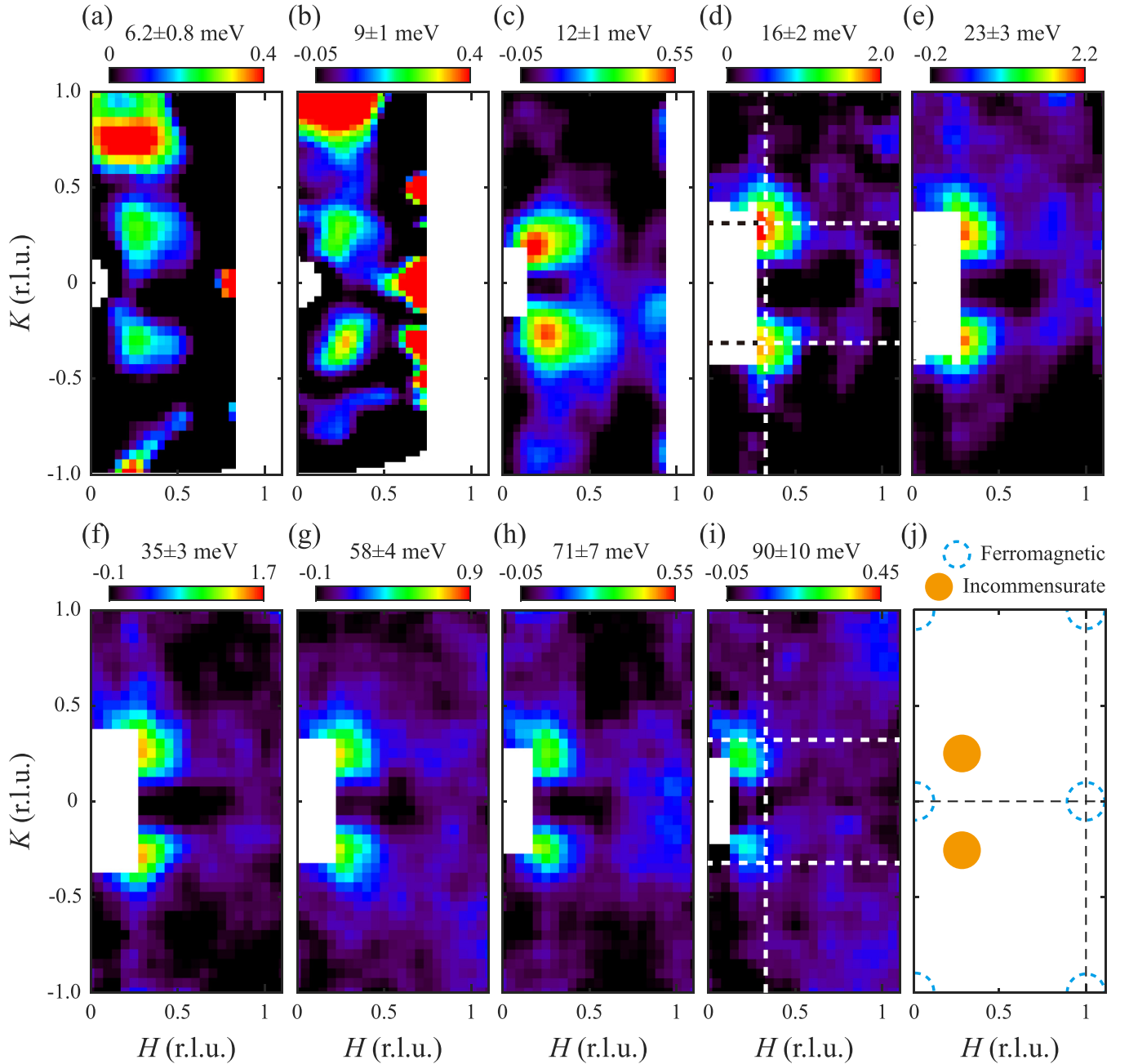


FIG. 2. Momentum dependence of the spin fluctuations in  $\text{Sr}_{1.8}\text{La}_{0.2}\text{RuO}_4$  at 5 K. Constant-energy images at indicated energies measured with incident neutron energies of  $E_i = 18.8$  (a) and (b), 40.2 (c), and 135.8 meV (d)–(i). Contour maps in (a) and (b) are rotated clockwise by  $90^\circ$  according to the  $C_4$  crystal symmetry for direct comparisons with data collected with higher incident energies. Data are symmetrized with respect to the  $K$  axis to enhance statistical accuracy and the  $|\mathbf{Q}|$ -dependent background is subtracted following the method introduced in Ref. [55]. Color bars indicate intensity in unit of  $\text{mbarn sr}^{-1} \text{meV}^{-1} \text{f.u.}^{-1}$ . Dashed lines in (d) and (i) mark the momenta with  $H = 0.3$  and  $K = \pm 0.3$ . The antiferromagnetic signals at 90 meV locate clearly at smaller wave vectors. (j) Schematic representation of the incommensurate antiferromagnetic and ferromagnetic wave vectors in the  $(H, K)$  plane.

non-negligible change to the low-energy dispersion of the  $\alpha$  and  $\beta$  bands that slightly departs from the rigid-band shift assumption [45]. Note that since the energy transfer is coupled to  $L$  in the time-of-flight scattering geometry, the  $E$ - $K$  contour plot yields no observable  $L$  modulation of the spin fluctuations.

We made constant-energy cuts through  $\mathbf{Q} = (0.3, 0.3)$  and  $(1, 0)$  to quantify the spin fluctuations. As shown in Figs. 4(a)–

4(j), the intensity of antiferromagnetic fluctuations displays a maximum at around 16 meV and gradually vanishes above 110 meV. The peak position shifts to a lower  $\mathbf{Q}$  with increasing energy in a nearly linear fashion [Figs. 3 and 4(j)]. A careful survey of the scattering intensity has been done around ferromagnetic wave vectors  $(1, 0)$  and  $(1, 1)$ . However, scans in the  $(1, K)$  direction covering these wave vectors are featureless at all energies [Fig. 4(k)], implying that ferromagnetic

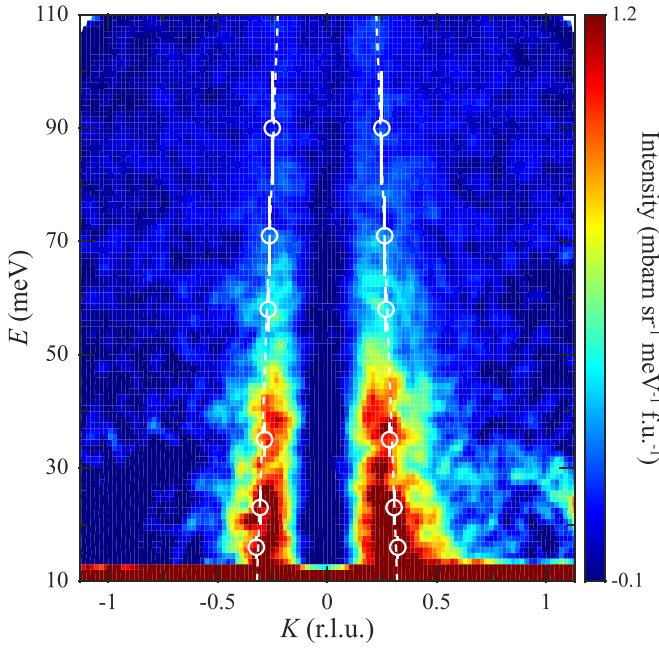


FIG. 3. Dispersion of the incommensurate spin fluctuations in  $\text{Sr}_{1.8}\text{La}_{0.2}\text{RuO}_4$  at 5 K measured with  $E_i = 135.8$  meV. Data are two-fold symmetrized with respect to the  $K$  axis and  $|\mathbf{Q}|$ -dependent backgrounds have been subtracted. The intensity is integrated from  $H = 0.1$  to  $0.5$ . Open circles denote peak positions extracted from Gaussian fits of constant-energy scans in Figs. 4(d)–4(i). Vertical bars indicate the energy integration range and the white dashed lines are linear fits to the peak positions.

fluctuations, if they exist, are still below the detection limit of the current INS instrument. This is further confirmed by our triple-axis measurements (see Fig. S3. in the Supplemental Material [54]).

Previous polarized neutron scattering measurements revealed relatively weak ferromagnetic fluctuations in  $\text{Sr}_2\text{RuO}_4$  [38,41,43]. These studies, however, were not able to distinguish whether the ferromagnetic fluctuations originate from itinerant electrons or local moments. Tight-binding calculations predict a divergence of bare band susceptibility  $\chi_0$  and an even more pronounced enhancement of the renormalized susceptibility  $\chi$ , when La doping pushes the vHS to the Fermi level and induces a divergence of the density of states in the  $\gamma$  band [44,45]. Indications of such enhanced electronic density of states were indeed observed by transport, specific heat and de Haas-van Alphen oscillations measurements [45,48]. Our data, however, reveal no discernible signal around the ferromagnetic wave vectors  $\mathbf{Q} = (1, 0)$  and  $(1, 1)$  at all energies measured, contradicting this weak-coupling scenario. Alternatively, the magnetic response around  $\Gamma$  point with a broad momentum distribution has been interpreted as quasilocal fluctuations driven by Hund's coupling in the DMFT calculation [46]. The absence of a sharp enhancement of the ferromagnetic fluctuations in  $\text{Sr}_{1.8}\text{La}_{0.2}\text{RuO}_4$  seems in favor of such a proposal. Interestingly, a recent angle-resolved photoemission measurement on the monolayer  $\text{SrRuO}_3$  film

also suggested that the vHS in the  $\gamma$  band does not lead to ferromagnetism but results in a strongly correlated metal state [58]. This is in line with current neutron scattering results in bulk  $\text{Sr}_{1.8}\text{La}_{0.2}\text{RuO}_4$ .

The prevalent paradigm of a  $p$ -wave triplet pairing state involves the exchange of bosonic ferromagnetic modes, while antiferromagnetic fluctuations favor a singlet pairing. The lack of conventional dispersive ferromagnetic fluctuations in  $\text{Sr}_2\text{RuO}_4$  seems to make it less likely to host a simple  $p$ -wave pairing than other candidates, where substantial well-defined ferromagnetic fluctuations have been observed, such as the heavy Fermion superconductor  $\text{UCoGe}$  [59] and iron-based compound  $\text{YFe}_2\text{Ge}_2$  [60]. Recent theoretical and experimental works have suggested composite order parameters in  $\text{Sr}_2\text{RuO}_4$  [19–23,25], which may involve multiple spin fluctuation pairing channels. Sophisticated theoretical calculations considering both antiferromagnetic and quasilocal ferromagnetic fluctuations on the Cooper pairing are highly desirable.

In summary, we used INS experiments to investigate spin fluctuations in  $\text{Sr}_{1.8}\text{La}_{0.2}\text{RuO}_4$  covering a broad range of energy-momentum space. Strong antiferromagnetic spin fluctuations emanate from the incommensurate position  $(0.3, 0.3)$ . The excitation extends to above 110 meV and progressively shifts to  $(0.25, 0.25)$ . On the other hand, there is no clearly increased scattering near ferromagnetic wave vectors. This contradicts the weak-coupling hypothesis, which predicts a divergence of ferromagnetic susceptibility as the vHS approaches Fermi level at this La doping. Instead, the inertia of weak ferromagnetic fluctuations against La doping is in line with the description of quasilocal fluctuations driven by Hund's coupling [46]. These results are crucial for a complete understanding of the magnetism in this system, and they set significant restrictions on the mechanism of superconductivity in  $\text{Sr}_2\text{RuO}_4$ .

This work was supported by the Key Program of the National Natural Science Foundation of China (Grant No. 12234006), the National Key R&D Program of China (Grant No. 2022YFA1403202), and the Shanghai Municipal Science and Technology Major Project (Grant No. 2019SHZDZX01). Q.W. was supported by the CUHK Research Startup Fund (Grant No. 4937150). Y.F. was supported by Xie Jialin Youth Foundation of Institute of High Energy Physics (Grant No. E2546JU2), and National Key R&D Program of China (Grant No. 2022YFA1604104). H.W. acknowledges support from the China National Postdoctoral Program for Innovative Talents (Grant No. BX2021080), China Postdoctoral Science Foundation (Grant No. 2021M700860), the Youth Foundation of the National Natural Science Foundation of China (Grant No. 12204108), and Shanghai Post-doctoral Excellence Program (Grant No. 2021481). The work at SNU was supported by the Institute for Basic Science in Korea (Grant No. IBS-R009-G2). D.T.A. thanks EPSRC-UK (Grant No. EP/W00562X/1). Experiments at PANDA were conducted under proposal numbers 5114 and 5719. Datasets collected at MERLIN spectrometer are available from the ISIS facility, Rutherford Appleton Laboratory data portal [61].



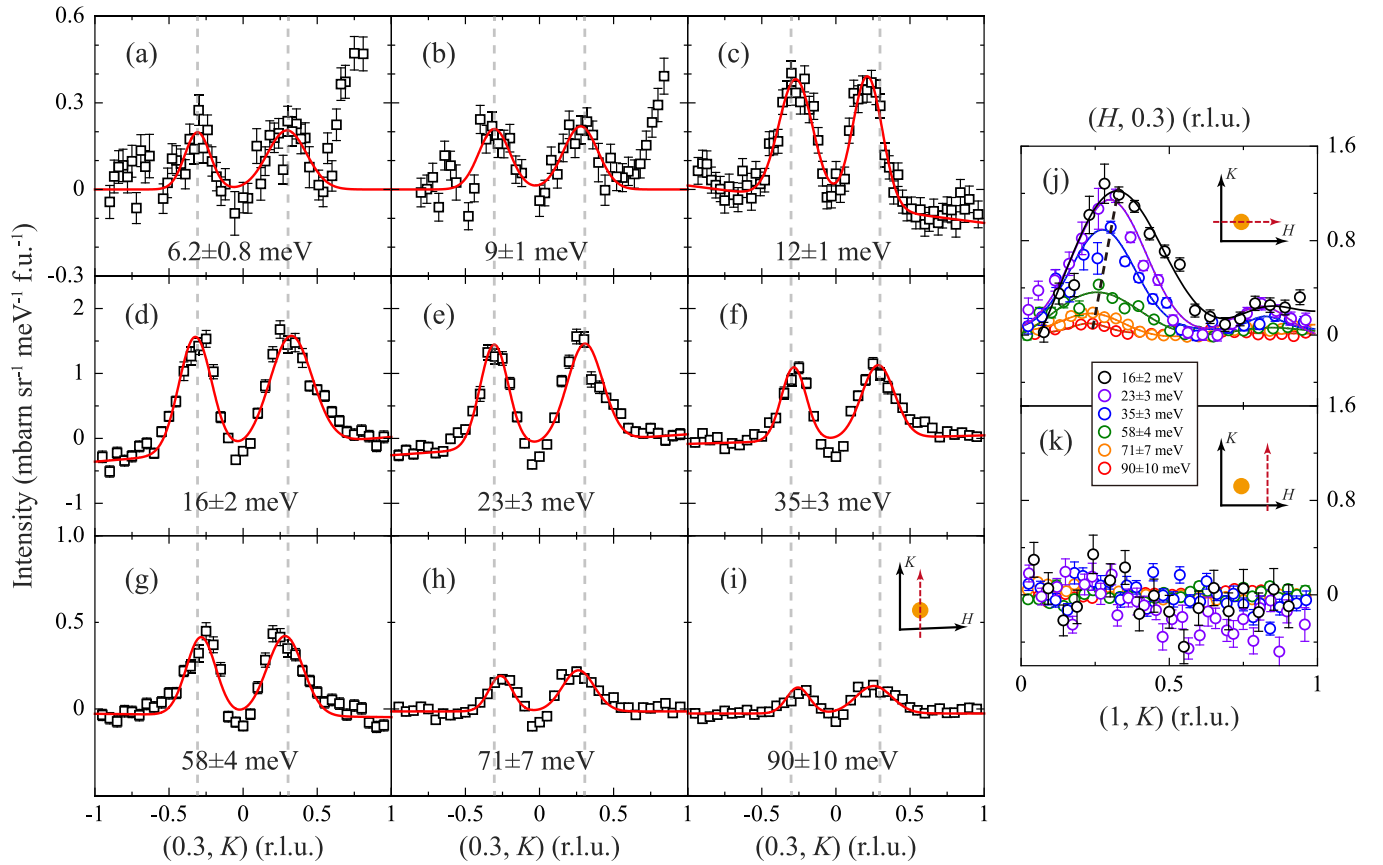


FIG. 4. Constant-energy scans of the spin fluctuations in  $\text{Sr}_{1.8}\text{La}_{0.2}\text{RuO}_4$  at 5 K. (a) and (b), (c), and (d)–(k) were collected on MERLIN with  $E_i = 18.8, 40.2$ , and  $135.8$  meV, respectively. (a)–(i) Constant-energy scans along  $(0.3, K)$  direction at indicated energies.  $H$  is integrated from  $0.05$  to  $0.55$ . Red solid curves are fits with two Gaussian profiles and a linear background. The fitted peak positions are plotted in Fig. 3. Gray dashed lines indicate  $K = \pm 0.3$ . (j) Constant-energy scans along  $(H, 0.3)$  direction with  $K$  integrated from  $0.10$  to  $0.50$ . Solid lines are fits with Gaussian profiles. (k) Constant-energy scans along  $(1, K)$  direction with  $H$  integrated from  $0.95$  to  $1.05$ . Data in (j) and (k) are symmetrized with respect to the  $K, H$  axes and the  $(1, 1)$  direction to enhance statistics. Backgrounds have been subtracted as described in Ref. [55]. The black dashed line connects the fitted peak positions at  $16$  and  $90$  meV. Arrows in the insets indicate the scan directions. Error bars represent one standard deviation.

- [1] A. P. Mackenzie and Y. Maeno, The superconductivity of  $\text{Sr}_2\text{RuO}_4$  and the physics of spin-triplet pairing, *Rev. Mod. Phys.* **75**, 657 (2003).
- [2] Y. Maeno, S. Kittaka, T. Nomura, S. Yonezawa, and K. Ishida, Evaluation of spin-triplet superconductivity in  $\text{Sr}_2\text{RuO}_4$ , *J. Phys. Soc. Jpn.* **81**, 011009 (2012).
- [3] C. Kallin and J. Berlinsky, Chiral superconductors, *Rep. Prog. Phys.* **79**, 054502 (2016).
- [4] A. P. Mackenzie, T. Scaffidi, C. W. Hicks, and Y. Maeno, Even odder after twenty-three years: The superconducting order parameter puzzle of  $\text{Sr}_2\text{RuO}_4$ , *npj Quantum Mater.* **2**, 40 (2017).
- [5] T. M. Rice and M. Sigrist,  $\text{Sr}_2\text{RuO}_4$ : An electronic analogue of  $^3\text{He}$ ?, *J. Phys.: Condens. Matter* **7**, L643 (1995).
- [6] G. Baskaran, Why is  $\text{Sr}_2\text{RuO}_4$  not a high  $T_c$  superconductor? Electron correlation, Hund's coupling and p-wave instability, *Phys. B: Condens. Matter* **223-224**, 490 (1996).
- [7] S. Raghu, A. Kapitulnik, and S. A. Kivelson, Hidden Quasi-One-Dimensional Superconductivity in  $\text{Sr}_2\text{RuO}_4$ , *Phys. Rev. Lett.* **105**, 136401 (2010).
- [8] K. Ishida, H. Mukuda, Y. Kitaoka, K. Asayama, Z. Q. Mao, Y. Mori, and Y. Maeno, Spin-triplet superconductivity in  $\text{Sr}_2\text{RuO}_4$  identified by  $^{17}\text{O}$  knight shift, *Nature (London)* **396**, 658 (1998).
- [9] J. A. Duffy, S. M. Hayden, Y. Maeno, Z. Mao, J. Kulda, and G. J. McIntyre, Polarized-Neutron Scattering Study of the Cooper-Pair Moment in  $\text{Sr}_2\text{RuO}_4$ , *Phys. Rev. Lett.* **85**, 5412 (2000).
- [10] G. M. Luke, Y. Fudamoto, K. M. Kojima, M. I. Larkin, J. Merrin, B. Nachumi, Y. J. Uemura, Y. Maeno, Z. Q. Mao, Y. Mori, H. Nakamura, and M. Sigrist, Time-reversal symmetry-breaking superconductivity in  $\text{Sr}_2\text{RuO}_4$ , *Nature (London)* **394**, 558 (1998).
- [11] J. Xia, Y. Maeno, P. T. Beyersdorf, M. M. Fejer, and A. Kapitulnik, High Resolution Polar Kerr Effect Measurements of  $\text{Sr}_2\text{RuO}_4$ : Evidence for Broken Time-Reversal Symmetry in the Superconducting State, *Phys. Rev. Lett.* **97**, 167002 (2006).
- [12] J. R. Kirtley, C. Kallin, C. W. Hicks, E.-A. Kim, Y. Liu, K. A. Moler, Y. Maeno, and K. D. Nelson, Upper limit on spontaneous supercurrents in  $\text{Sr}_2\text{RuO}_4$ , *Phys. Rev. B* **76**, 014526 (2007).

- [13] C. W. Hicks, J. R. Kirtley, T. M. Lippman, N. C. Koshnick, M. E. Huber, Y. Maeno, W. M. Yuhasz, M. B. Maple, and K. A. Moler, Limits on superconductivity-related magnetization in  $\text{Sr}_2\text{RuO}_4$  and  $\text{PrOs}_4\text{Sb}_{12}$  from scanning SQUID microscopy, *Phys. Rev. B* **81**, 214501 (2010).
- [14] S. Kittaka, T. Nakamura, Y. Aono, S. Yonezawa, K. Ishida, and Y. Maeno, Angular dependence of the upper critical field of  $\text{Sr}_2\text{RuO}_4$ , *Phys. Rev. B* **80**, 174514 (2009).
- [15] C. W. Hicks, D. O. Brodsky, E. A. Yelland, A. S. Gibbs, J. A. N. Bruin, M. E. Barber, S. D. Edkins, K. Nishimura, S. Yonezawa, Y. Maeno, and A. P. Mackenzie, Strong increase of  $T_c$  of  $\text{Sr}_2\text{RuO}_4$  under both tensile and compressive strain, *Science* **344**, 283 (2014).
- [16] A. Pustogow, Y. Luo, A. Chronister, Y.-S. Su, D. A. Sokolov, F. Jerzembeck, A. P. Mackenzie, C. W. Hicks, N. Kikugawa, S. Raghu, E. D. Bauer, and S. E. Brown, Constraints on the superconducting order parameter in  $\text{Sr}_2\text{RuO}_4$  from oxygen-17 nuclear magnetic resonance, *Nature (London)* **574**, 72 (2019).
- [17] K. Ishida, M. Manago, K. Kinjo, and Y. Maeno, Reduction of the  $^{17}\text{O}$  knight shift in the superconducting state and the heat-up effect by NMR pulses on  $\text{Sr}_2\text{RuO}_4$ , *J. Phys. Soc. Jpn.* **89**, 034712 (2020).
- [18] A. N. Petsch, M. Zhu, M. Enderle, Z. Q. Mao, Y. Maeno, I. I. Mazin, and S. M. Hayden, Reduction of the Spin Susceptibility in the Superconducting State of  $\text{Sr}_2\text{RuO}_4$  observed by Polarized Neutron Scattering, *Phys. Rev. Lett.* **125**, 217004 (2020).
- [19] S. Benhabib, C. Lupien, I. Paul, L. Berges, M. Dion, M. Nardone, A. Zitouni, Z. Q. Mao, Y. Maeno, A. Georges, L. Taillefer, and C. Proust, Ultrasound evidence for a two-component superconducting order parameter in  $\text{Sr}_2\text{RuO}_4$ , *Nat. Phys.* **17**, 194 (2021).
- [20] S. Ghosh, A. Shekhter, F. Jerzembeck, N. Kikugawa, D. A. Sokolov, M. Brando, A. P. Mackenzie, C. W. Hicks, and B. J. Ramshaw, Thermodynamic evidence for a two-component superconducting order parameter in  $\text{Sr}_2\text{RuO}_4$ , *Nat. Phys.* **17**, 199 (2021).
- [21] V. Grinenko, S. Ghosh, R. Sarkar, J.-C. Orain, A. Nikitin, M. Elender, D. Das, Z. Guguchia, F. Brückner, M. E. Barber, J. Park, N. Kikugawa, D. A. Sokolov, J. S. Bobowski, T. Miyoshi, Y. Maeno, A. P. Mackenzie, H. Luetkens, C. W. Hicks, and H.-H. Klauss, Split superconducting and time-reversal symmetry-breaking transitions in  $\text{Sr}_2\text{RuO}_4$  under stress, *Nat. Phys.* **17**, 748 (2021).
- [22] V. Grinenko, D. Das, R. Gupta, B. Zinkl, N. Kikugawa, Y. Maeno, C. W. Hicks, H.-H. Klauss, M. Sgrist, and R. Khasanov, Unsplit superconducting and time reversal symmetry breaking transitions in  $\text{Sr}_2\text{RuO}_4$  under hydrostatic pressure and disorder, *Nat. Commun.* **12**, 3920 (2021).
- [23] S. A. Kivelson, A. C. Yuan, B. Ramshaw, and R. Thomale, A proposal for reconciling diverse experiments on the superconducting state in  $\text{Sr}_2\text{RuO}_4$ , *npj Quantum Mater.* **5**, 43 (2020).
- [24] R. Sharma, S. D. Edkins, Z. Wang, A. Kostin, C. Sow, Y. Maeno, A. P. Mackenzie, J. C. S. Davis, and V. Madhavan, Momentum-resolved superconducting energy gaps of  $\text{Sr}_2\text{RuO}_4$  from quasiparticle interference imaging, *Proc. Natl. Acad. Sci.* **117**, 5222 (2020).
- [25] A. T. Rømer, D. D. Scherer, I. M. Eremin, P. J. Hirschfeld, and B. M. Andersen, Knight Shift and Leading Superconducting Instability from Spin Fluctuations in  $\text{Sr}_2\text{RuO}_4$ , *Phys. Rev. Lett.* **123**, 247001 (2019).
- [26] H. S. Røising, T. Scaffidi, F. Flicker, G. F. Lange, and S. H. Simon, Superconducting order of  $\text{Sr}_2\text{RuO}_4$  from a three-dimensional microscopic model, *Phys. Rev. Res.* **1**, 033108 (2019).
- [27] H. G. Suh, H. Menke, P. M. R. Brydon, C. Timm, A. Ramires, and D. F. Agterberg, Stabilizing even-parity chiral superconductivity in  $\text{Sr}_2\text{RuO}_4$ , *Phys. Rev. Res.* **2**, 032023 (2020).
- [28] M. Braden, O. Friedt, Y. Sidis, P. Bourges, M. Minakata, and Y. Maeno, Incommensurate Magnetic Ordering in  $\text{Sr}_2\text{Ru}_{1-x}\text{Ti}_x\text{O}_4$ , *Phys. Rev. Lett.* **88**, 197002 (2002).
- [29] J. P. Carlo, T. Goko, I. M. Gat-Malureanu, P. L. Russo, A. T. Savici, A. A. Aczel, G. J. MacDougall, J. A. Rodriguez, T. J. Williams, G. M. Luke, C. R. Wiebe, Y. Yoshida, S. Nakatsuji, Y. Maeno, T. Taniguchi, and Y. J. Uemura, New magnetic phase diagram of  $(\text{Sr}, \text{Ca})_2\text{RuO}_4$ , *Nat. Mater.* **11**, 323 (2012).
- [30] J. E. Ortmann, J. Y. Liu, J. Hu, M. Zhu, J. Peng, M. Matsuda, X. Ke, and Z. Q. Mao, Competition between antiferromagnetism and ferromagnetism in  $\text{Sr}_2\text{RuO}_4$  probed by Mn and Co doping, *Sci. Rep.* **3**, 2950 (2013).
- [31] I. I. Mazin and D. J. Singh, Ferromagnetic Spin Fluctuation Induced Superconductivity in  $\text{Sr}_2\text{RuO}_4$ , *Phys. Rev. Lett.* **79**, 733 (1997).
- [32] I. I. Mazin and D. J. Singh, Competitions in Layered Ruthenates: Ferromagnetism Versus Antiferromagnetism and Triplet Versus Singlet Pairing, *Phys. Rev. Lett.* **82**, 4324 (1999).
- [33] P. Monthoux and G. G. Lonzarich,  $p$ -wave and  $d$ -wave superconductivity in quasi-two-dimensional metals, *Phys. Rev. B* **59**, 14598 (1999).
- [34] T. Kuwabara and M. Ogata, Spin-Triplet Superconductivity Due to Antiferromagnetic Spin-Fluctuation in  $\text{Sr}_2\text{RuO}_4$ , *Phys. Rev. Lett.* **85**, 4586 (2000).
- [35] J.-W. Huo, T. M. Rice, and F.-C. Zhang, Spin Density Wave Fluctuations and  $p$ -Wave Pairing in  $\text{Sr}_2\text{RuO}_4$ , *Phys. Rev. Lett.* **110**, 167003 (2013).
- [36] Y. Sidis, M. Braden, P. Bourges, B. Hennion, S. NishiZaki, Y. Maeno, and Y. Mori, Evidence for Incommensurate Spin Fluctuations in  $\text{Sr}_2\text{RuO}_4$ , *Phys. Rev. Lett.* **83**, 3320 (1999).
- [37] M. Braden, Y. Sidis, P. Bourges, P. Pfeuty, J. Kulda, Z. Mao, and Y. Maeno, Inelastic neutron scattering study of magnetic excitations in  $\text{Sr}_2\text{RuO}_4$ , *Phys. Rev. B* **66**, 064522 (2002).
- [38] M. Braden, P. Steffens, Y. Sidis, J. Kulda, P. Bourges, S. Hayden, N. Kikugawa, and Y. Maeno, Anisotropy of the Incommensurate Fluctuations in  $\text{Sr}_2\text{RuO}_4$ : A study with Polarized Neutrons, *Phys. Rev. Lett.* **92**, 097402 (2004).
- [39] K. Iida, M. Kofu, N. Katayama, J. Lee, R. Kajimoto, Y. Inamura, M. Nakamura, M. Arai, Y. Yoshida, M. Fujita, K. Yamada, and S.-H. Lee, Inelastic neutron scattering study of the magnetic fluctuations in  $\text{Sr}_2\text{RuO}_4$ , *Phys. Rev. B* **84**, 060402(R) (2011).
- [40] S. Kunkemöller, P. Steffens, P. Link, Y. Sidis, Z. Q. Mao, Y. Maeno, and M. Braden, Absence of a Large Superconductivity-Induced Gap in Magnetic Fluctuations of  $\text{Sr}_2\text{RuO}_4$ , *Phys. Rev. Lett.* **118**, 147002 (2017).
- [41] P. Steffens, Y. Sidis, J. Kulda, Z. Q. Mao, Y. Maeno, I. I. Mazin, and M. Braden, Spin Fluctuations in  $\text{Sr}_2\text{RuO}_4$  from Polarized Neutron Scattering: Implications for Superconductivity, *Phys. Rev. Lett.* **122**, 047004 (2019).
- [42] K. Iida, M. Kofu, K. Suzuki, N. Murai, S. Ohira-Kawamura, R. Kajimoto, Y. Inamura, M. Ishikado, S. Hasegawa, T. Masuda, Y. Yoshida, K. Kakurai, K. Machida, and S. Lee, Horizontal line

- nodes in  $\text{Sr}_2\text{RuO}_4$  proved by spin resonance, *J. Phys. Soc. Jpn.* **89**, 053702 (2020).
- [43] K. Jenni, S. Kunkemöller, P. Steffens, Y. Sidis, R. Bewley, Z. Q. Mao, Y. Maeno, and M. Braden, Neutron scattering studies on spin fluctuations in  $\text{Sr}_2\text{RuO}_4$ , *Phys. Rev. B* **103**, 104511 (2021).
- [44] C. Bergemann, A. P. Mackenzie, S. R. Julian, D. Forsythe, and E. Ohmichi, Quasi-two-dimensional Fermi liquid properties of the unconventional superconductor  $\text{Sr}_2\text{RuO}_4$ , *Adv. Phys.* **52**, 639 (2003).
- [45] N. Kikugawa, C. Bergemann, A. P. Mackenzie, and Y. Maeno, Band-selective modification of the magnetic fluctuations in  $\text{Sr}_2\text{RuO}_4$ : A study of substitution effects, *Phys. Rev. B* **70**, 134520 (2004).
- [46] H. U. R. Strand, M. Zingl, N. Wentzell, O. Parcollet, and A. Georges, Magnetic response of  $\text{Sr}_2\text{RuO}_4$ : Quasi-local spin fluctuations due to Hund's coupling, *Phys. Rev. B* **100**, 125120 (2019).
- [47] K. M. Shen, N. Kikugawa, C. Bergemann, L. Balicas, F. Baumberger, W. Meevasana, N. J. C. Ingle, Y. Maeno, Z.-X. Shen, and A. P. Mackenzie, Evolution of the Fermi Surface and Quasiparticle Renormalization Through a Van Hove Singularity in  $\text{Sr}_{2-y}\text{La}_y\text{RuO}_4$ , *Phys. Rev. Lett.* **99**, 187001 (2007).
- [48] N. Kikugawa, A. P. Mackenzie, C. Bergemann, R. A. Borzi, S. A. Grigera, and Y. Maeno, Rigid-band shift of the Fermi level in the strongly correlated metal:  $\text{Sr}_{2-y}\text{La}_y\text{RuO}_4$ , *Phys. Rev. B* **70**, 060508(R) (2004).
- [49] B. Burganov, C. Adamo, A. Mulder, M. Uchida, P. D. C. King, J. W. Harter, D. E. Shai, A. S. Gibbs, A. P. Mackenzie, R. Uecker, M. Bruetzmann, M. R. Beasley, C. J. Fennie, D. G. Schlom, and K. M. Shen, Strain Control of Fermiology and Many-Body Interactions in Two-Dimensional Ruthenates, *Phys. Rev. Lett.* **116**, 197003 (2016).
- [50] A. Steppke, L. Zhao, M. E. Barber, T. Scaffidi, F. Jerzembeck, H. Rosner, A. S. Gibbs, Y. Maeno, S. H. Simon, A. P. Mackenzie, and C. W. Hicks, Strong peak in  $T_c$  of  $\text{Sr}_2\text{RuO}_4$  under uniaxial pressure, *Science* **355**, eaaf9398 (2017).
- [51] M. E. Barber, A. S. Gibbs, Y. Maeno, A. P. Mackenzie, and C. W. Hicks, Resistivity in the Vicinity of a Van Hove Singularity:  $\text{Sr}_2\text{RuO}_4$  Under Uniaxial Pressure, *Phys. Rev. Lett.* **120**, 076602 (2018).
- [52] C. A. Marques, L. C. Rhodes, R. Fittipaldi, V. Granata, C. M. Yim, R. Buzio, A. Gerbi, A. Vecchione, A. W. Rost, and P. Wahl, Magnetic-field tunable intertwined checkerboard charge order and nematicity in the surface layer of  $\text{Sr}_2\text{RuO}_4$ , *Adv. Mater.* **33**, 2100593 (2021).
- [53] C. Kim, W. Kyung, S. Park, C. Leem, D. Song, Y. Kim, S. Choi, W. Jung, Y. Koh, H. Choi, Y. Yoshida, R. Moore, Z.-X. Shen, and C. Kim, Self-energy analysis of multiple-bosonic mode coupling in  $\text{Sr}_2\text{RuO}_4$ , *J. Phys. Chem. Solids* **72**, 556 (2011).
- [54] See Supplemental Material at <http://link.aps.org/supplemental/10.1103/PhysRevB.107.L201107> for detailed EPMA data, XRD and refinement results, INS measurements via triple-axis spectrometer and the representative raw data of INS experiments used in the main text. The Supplemental Material also contains Ref. [55].
- [55] Q. Wang, Y. Shen, B. Pan, X. Zhang, K. Ikeuchi, K. Iida, A. D. Christianson, H. C. Walker, D. T. Adroja, M. Abdel-Hafiez, X. Chen, D. A. Chareev, A. N. Vasiliev, and J. Zhao, Magnetic ground state of FeSe, *Nat. Commun.* **7**, 12182 (2016).
- [56] R. Bewley, R. Eccleston, K. McEwen, S. Hayden, M. Dove, S. Bennington, J. Treadgold, and R. Coleman, MERLIN, a new high count rate spectrometer at ISIS, *Phys. B: Condens. Matter* **385-386**, 1029 (2006).
- [57] A. Schneidewind and P. Čermák, PANDA: Cold three axes spectrometer, *J. Large Scale Res. Facil.* **1**, A12 (2015).
- [58] B. Sohn, J. R. Kim, C. H. Kim, S. Lee, S. Hahn, Y. Kim, S. Huh, D. Kim, Y. Kim, W. Kyung, M. Kim, M. Kim, T. W. Noh, and C. Kim, Observation of metallic electronic structure in a single-atomic-layer oxide, *Nat. Commun.* **12**, 6171 (2021).
- [59] C. Stock, D. A. Sokolov, P. Bourges, P. H. Tobash, K. Gofryk, F. Ronning, E. D. Bauer, K. C. Rule, and A. D. Huxley, Anisotropic Critical Magnetic Fluctuations in the Ferromagnetic Superconductor UCoGe, *Phys. Rev. Lett.* **107**, 187202 (2011).
- [60] H. Wo, Q. Wang, Y. Shen, X. Zhang, Y. Hao, Y. Feng, S. Shen, Z. He, B. Pan, W. Wang, K. Nakajima, S. Ohira-Kawamura, P. Steffens, M. Boehm, K. Schmalzl, T. R. Forrest, M. Matsuda, Y. Zhao, J. W. Lynn, Z. Yin *et al.*, Coexistence of Ferromagnetic and Stripe-Type Antiferromagnetic Spin Fluctuations in  $\text{YFe}_2\text{Ge}_2$ , *Phys. Rev. Lett.* **122**, 217003 (2019).
- [61] <https://doi.org/10.5286/ISIS.E.42581971>